JOURNAL OF AGRICULTURAL AND FOOD CHEMISTRY

Cooking Behavior of Rice in Relation to Kernel Physicochemical and Structural Properties

VÉRONIQUE VIDAL,[†] BRIGITTE PONS,[†] JUDITH BRUNNSCHWEILER,[‡] STEPHAN HANDSCHIN,[‡] XAVIER ROUAU,[§] AND CHRISTIAN MESTRES[†,*]

CIRAD, UPR Qualité des Aliments Tropicaux, 73 avenue J.F. Breton, 34398 Montpellier Cedex 5, France, Institute of Food Science and Nutrition, ETH Zürich, CH-8092 Zürich, Switzerland, and INRA-UMR Ingénierie des Agropolymères et Technologies Emergentes, 2 place Pierre Viala, 34060 Montpellier cedex 1, France

A set of 27 rice varieties were evaluated for their morphological grain characteristics (length, width, thickness, thousand kernel weight, TKW), chemical composition (amylose, protein, and ash content) and starch properties (gelatinization temperature and enthalpy, amylose−lipid complex). In addition, cell walls were characterized by the arabinoxylan and β-glucan contents. A rapid method for determining optimum rice cooking time was developed based on the swelling ratio; a fixed value of 2.55 gave a gelatinization level of 95% assessed by differential scanning calorimetry and translucence testing. Optimum cooking time appears positively correlated with kernel thickness and TKW but also with ash content. Confocal laser and scanning electron microscope observation of uncooked rice grains revealed different structural features (cell size) and fracture behavior: for some cultivars, the fracture showed ruptured cells, whereas for others most cells were intact. These structural differences, which may be linked to pectin content, could partly explain rice kernel cooking behavior.

KEYWORDS: Rice; cooking; structure; cell wall; starch properties

INTRODUCTION

Although rice is consumed worldwide, there is no universal rice quality attribute (*1*). But whatever the target market, cooked rice texture represents one of the main quality attributes (*2*, *3*). So measuring and understanding rice texture properties is a great challenge for the rice industry and breeders in meeting consumer demand.

Rice textural properties can depend on many characteristics, but also on the cooking method and degree. Standardization of cooking is therefore a prerequisite for the evaluation of cooked rice texture. The cooking end point, however, broadly varies in literature: some use the disappearance of the white core in excess water, whereas others use a fixed cooking time or fixed rice to water ratio (*4*, *5*).

Numerous studies aim at predicting rice cooking behavior (*5*, *6*). It is generally attempted to link cooking time and rice physicochemical characteristics. Kernel size and shape (particularly thickness) have been proved to be the major factors influencing cooking time, but rice with high protein and amylose contents also seem to have longer cooking times. There has been however relatively little consideration of the involvement of cell wall components, since they represent a minor constituent of the grain. A rice kernel can nevertheless be considered as a cellular solid, a pile of bricks (cells) whose shape, size, and composition may play a part in rice cooking behavior.

This study aims at investigating the cooking quality of milled rice varieties cultivated in France. The first stage was determining the optimal cooking time, with relationships between physicochemical characteristics, cell wall composition, and optimal cooking time being established. Microstructural observations are also presented to support the role of kernel structure in rice cooking behavior.

MATERIALS AND METHODS

Plant Material. Preliminary studies were made of six commercial milled rice samples. In addition, 21 cultivars (*japonica* subspecies) harvested in 2003 in experimental fields at the French Rice Center (Arles, France) were used. Paddy rice was stored in an air-conditioned room (20 °C, 65% RH) to reach a 12−13% water content equilibrium (wet basis, wb). Dehusking and polishing were carried out using a Satake testing husker (THU 35B, Satake Engineering Co., Tokyo) and an Olmia testing abrasive polisher (Vercelli, Italy), respectively. The milling degree ([1-(wt. of milled rice/wt. of brown rice)] × 100) was set to 12% for all cultivars. Raw milled rice was ground using a laboratory Mill (Perten) before chemical and thermal analyses.

Physical Characteristics of Raw Rice Kernels. One thousand head rice kernels were counted (Numigral seed counter, Tripette & Renaud, France) and weighed. The mean of two replications was calculated.

The length and width were determined by image analysis. A hundred milled rice kernels were spread on the glass plate of a flatbed scanner

* Correspondence with author: tel., 33 467 614 473; fax, 33 467 614 444; christian.mestres@cirad.fr.
[†] CIRAD, UPR Qualité des Aliments Tropicaux.
[‡] Institute of Food Science and Nutrition.
[§] INRA-UMR Ingénierie des Agropolymères et Technologies Emergentes.

10.1021/jf061945o CCC: $37.00
Published on Web 12/22/2006

(HP Scan Jet 6200C). Touching kernels were manually separated, and then they were all covered by a black paper sheet to amplify contrast between the objects (rice kernels) and background. The image was scanned in 8 bits grayscale with a resolution of 200 dpi using digital image analysis software (SigmaScanPro 5.0). A thresholding operation was applied to separate rice kernels from the background. The length (L, mm) was measured by searching for the farthest pixels of each kernel and the width (W, mm) by the largest distance of the object perpendicular to the major axis. The surface area was calculated from the number of pixels on each kernel. The mean value for 100 kernels was calculated. The thickness was manually measured using a gauge on 20 unbroken milled kernels and the mean value calculated.

Microscopy. Raw whole milled kernels were directly observed using an Olympus SZ PT stereomicroscope (DE Hamburg). Pictures were recorded digitally by a Hamamatsu C5810 video camera.

Fractures of raw whole milled kernels were observed by confocal laser scanning microscope (CLSM) or scanning electron microscope (SEM). In the first case, kernels were soaked in water for 2−3 h and then bent until the breaking point. They were then stained with acridin orange (0.02% v/v) for 10 min and then observed using a Leica TCS SP CLSM equipped with an inverted DM RXE fluorescence light optical microscope (Leica, Lasertechnik GmbH, DE-Heidelberg) working with a Ar/Kr laser. The excitation wavelength was 488 nm, and the emission was recorded between 500 and 580 nm. 3D image stacks were obtained in 2D projections, and image analyses were carried out with the NIH Image 1.6.2 software. In the second case, kernels were directly bent until the breaking point and fixed with Leit-C (carbon conductive cement) on aluminum stubs and sputter-coated with 5 nm platinum before observation under the scanning electron microscope (Zeiss, Gemini 1530, Germany-Oberkochen) at 5 kV with a working distance of 25 mm.

Chemical Analysis and Cell Wall Composition. Moisture content was determined by weighing before and after drying at 130 °C for 2 h. Protein content was calculated from nitrogen content assessed by the Kjeldhal method (Tecator Kjeltec, Sweden) using a 5.95 conversion factor. Ash content was measured after incineration at 500 °C for 8 h.

β-Glucans were determined using the mixed linkage β-glucan kit from Megazyme (Ireland). β-Glucans are broken down to glucose by the successive action of lichenase and β-glucosidase. The glucose produced was then tested using a glucose oxidase peroxidase reagent. Arabinoxylans were tested according to the procedure of Rouau and Surget (*7*). Analyses were performed in duplicate and results expressed in % (db).

Cooking Procedure and Swelling Ratio Determination. A quantity of 62.5 g of milled rice was put into a perforated plastic bag and cooked in 1 L of boiling spring water (Volvic, France) containing 3.5 g of sodium chloride. Just after complete cooking, the perforated plastic bag was rapidly taken out of the boiling water, the water drained off for 1 min and the bag weighed. Swelling ratio (SR) was defined as the ratio of cooked to original rice weight.

Assessment of Rice Kernel Degree of Translucence. Eight cooked rice kernels were pressed between two glass slides (8 cm wide). The operation was replicated four times, with the four slides placed on the glass plate of the scanner and covered with a black sheet of paper. The image was scanned in 8 bits grayscale with a resolution of 300 dpi. The scanned image (**Figure 1**a) was submitted to two threshold processes: the first one selecting the total area of pressed crushed kernels (**Figure 1b**) and the second selecting only white cores (**Figure 1c**). The degree of translucence (% *T*) was calculated on each binary image:

$$\% T = [1 - (\text{area}_{WC}/\text{area}_{K})] \times 100$$

where area_{WC} = area of white core in the 32 pressed kernels, and area_{K} = total area of pressed kernels.

Thermal Analysis. The amylose content was determined on raw rice samples from the measurement of the energy of amylose/lysophospholipid complex formation using differential scanning calorimetry (DSC 7 Perkin-Elmer, Norwalk, CT) as per Mestres et al. (*8*). In addition, the onset temperature (T_o) and enthalpy change (ΔH, J/g) of the heating thermal transitions (gelatinization and amylose/lipid complex fusion) were determined using a slightly modified procedure. Rice flour (10 mg) was accurately weighed into a stainless steel pan, and 50 μL of ultrapure water was added. After being sealed, the pan was heated from 25 °C to 140 °C (against an empty pan): gelatinization was observed between 50 and 90 °C and amylose−lipid complex fusion above 100 °C.

The enthalpy change due to gelatinization was also assessed on cooked rice samples which were predried at 50 °C for 48 h and then ground. The ratio of starch gelatinization enthalpy change after cooking (ΔH cooked) to before cooking (ΔH raw) was used to calculate the cooked rice starch gelatinization percentage (% G):

$$\% G = [1 - (\Delta H_{\text{cooked}}/\Delta H_{\text{raw}})] \times 100$$

Statistical Analysis. Histogram plots, principal component analysis, and multiple regressions were performed using Statistica 7.1 (Statsoft, Tulsa, OK).

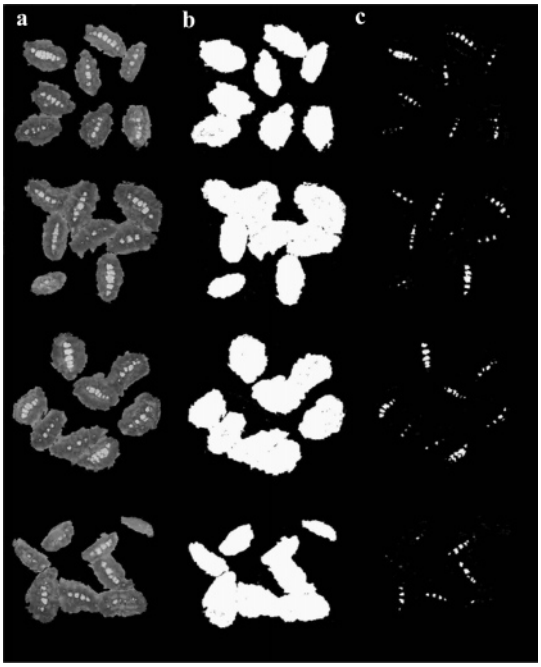

Figure 1. (a) Grayscale image of 32 crushed kernels between two glasses. (b) Binary image with a threshold selecting the overall area. (c) Binary image with a threshold selecting the white cores.

Table 1. Characteristics of Commercial Rice Varieties

	morphology				
variety	grain type[a]	*L* (mm)	*W* (mm)	*L*/*W*	amylose (% db)
Thaibonnet	long B	7.11	2.06	3.45	23.9
Thai	long B	6.86	2.04	3.36	13.9
Basmati	long B	6.85	1.77	3.88	22.8
Surinam	long B	7.73	2.30	3.36	23.4
Ariete	long A	6.22	2.55	2.44	18.4
Selenio	short	3.96	2.88	1.38	18.8

[a] According to EEC classification *L*: length; *W*: width.

RESULTS

Preliminary Study on Commercial Rice Varieties: Determining Optimum Cooking Time. The preliminary study aimed to develop a procedure for determining the optimum cooking time. Six commercial rice varieties were used, representative of rice variability as far as possible, especially in terms of their morphological characteristics and amylose content (**Table 1**). Under EEC commercial classification, four varieties belonged to "long B" type (length/width ≥3 and grain length

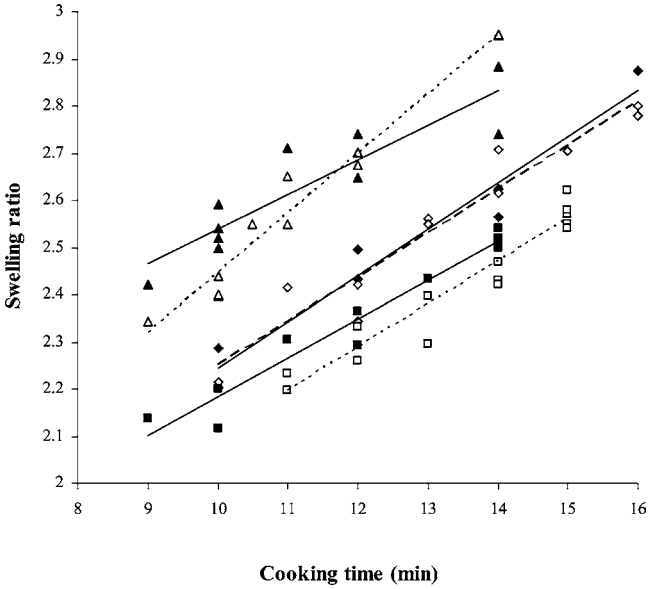

Figure 2. Evolution of the swelling ratio with cooking time for Thaibonnet (◆), Basmati (▲), Thai (△), Surinam (◇), Ariete (□), and Slenio (■).

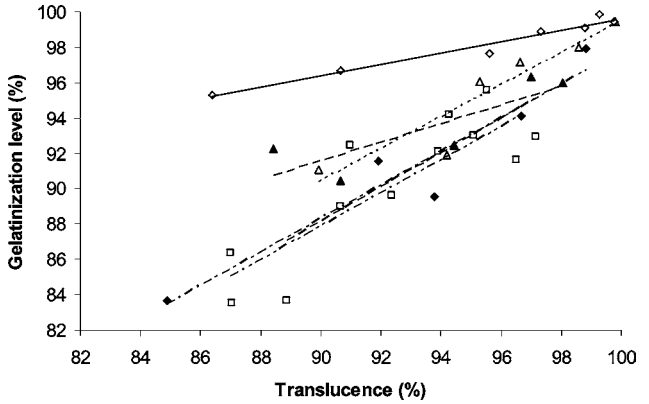

Figure 3. Relationship between translucence and starch gelatinization level percentages for Thaibonnet (◆), Basmati (▲), Thai (△), Surinam (◇), Ariete (□), and Slenio (■).

>6 mm), one to "long A" type (2 < length/width <3 and grain length >6 mm) and one to "short" type (length/width <2 and grain length ≤5.2 mm). Amylose content ranged from 13.9% (dry basis, db) for Thai to 23.9% (db) for Thaibonnet.

Swelling ratio was monitored as a function of cooking duration (from 9 to 16 min; **Figure 2**). It showed a linear increase against cooking time for all varieties but was higher for Basmati and Thai (slender varieties, **Table 1**) and lower for Ariete and Selenio (wider varieties).

The cooking degree of rice was evaluated by the percentage starch gelatinization measured by DSC and by the translucence percentage of pressed kernels measured by image analysis. The correlation between the gelatinization level and translucent area (%) was highly significant, varying from 0.78 for Ariete to 0.98 for Surinam (**Figure 3**): a translucence value of 95% corresponded to a gelatinization degree ranging from 92 to 95%. Surinam exhibited a slightly different figure, with a higher gelatinization degree than translucence value: it was for example of 98% with a translucence of 95%. It appears nevertheless that translucence is a rapid and fairly accurate procedure for evaluating starch gelatinization (with a standard estimate error ranging from 0.4 to 2.8) and hence rice cooking level.

The relationship between translucence rate and swelling ratio is presented in **Figure 4**. Complete disappearance of chalky

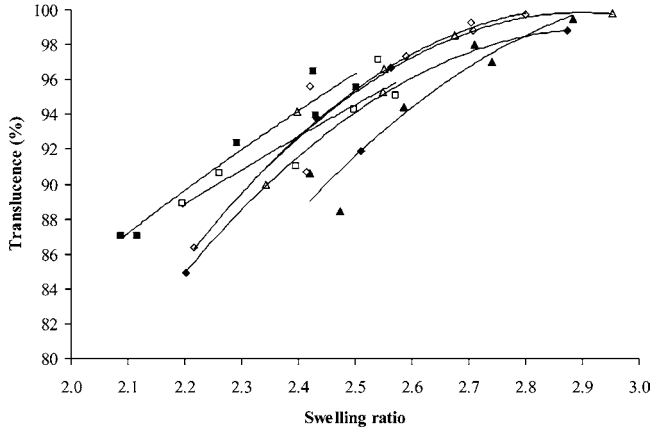

Figure 4. Evolution of translucence percentage as a function of swelling ratio during cooking of Thaibonnet (◆), Basmati (▲), Thai (△), Surinam (◇), Ariete (□), and Slenio (■).

Table 2. Cooking Time and Gelatinization Level of Commercial Rice Varieties

variety	cooking time (min)	swelling ratio	gelatinization level	
			DSC[a]	translucence
Thaibonnet	12.0	2.49	89.8	92.8
Thai	10.0	2.55	93.3	91.4
Basmati	10.5	2.55	96.2	95.3
Surinam	13.0	2.58	99.0	97.3
Ariete	15.0	2.53	94.9	96.2
Selenio	14.0	2.47	94.8	96.0
mean value		2.53	94.7	94.8

[a] DSC: differential scanning calorimetry.

cores was achieved at a swelling ratio around 3.0 whereas a translucence value of 95% was attained with a swelling ratio ranging from 2.45 to 2.65. Optimum cooking time was thus estimated from the swelling ratio curve at 2.55. So the six commercial rice samples were cooked for their specific optimum cooking time: the mean swelling ratio was 2.53 whereas the mean gelatinization and translucence values were 94.7 and 94.8%, respectively (**Table 2**).

This preliminary study (on a limited rice sample) showed that a rapid procedure can be used to evaluate rice cooking time: it is the time required to attain a swelling ratio of 2.55. This condition achieved a starch gelatinization level of 95%. This procedure would be used for the entire sample.

Physicochemical Characteristics and Cooking Time of the 27 Rice Varieties. Table 3 lists the physicochemical properties of the 27 rice samples arranged by class format: the commercial samples are listed in the first six lines. The majority (*20*) had long grains and belonged to long B type, whereas four belonged to the long A type and three to the short grain type. The thousand kernel weight (TKW) ranged from 16 to 24 g except for four samples which had TKW over 26 g; three of them were long A-type rice. Protein content ranged from 5.6 to 10.5% (db), with the majority between 7 and 8%. Amylose content ranged from 13 to 26.5% (db) with 10 rice samples around 15% and the others scattered between 20 and 28% (**Figure 5**a). Large variations were observed in the gelatinization onset temperature (T_o, 57.4−74 °C) and enthalpy (10.5−15.5 J/g db) (**Figure 5b**,**c**). Two populations were revealed for T_o values of around 60−65 and 70−75 °C, respectively. Short grains typically exhibited low to intermediate amylose content (14.7−18.8% db) and a relatively low gelatinization temperature (57.4−64.9 °C). The long-grain class was more dispersed, encompassing rice

Table 3. Physicochemical Characteristics of the 27 Rice Varieties[a]

	morphology						
variety	*L* (mm)	*W* (mm)	*T* (mm)	*L*/*W*	type	TKW (g db)	CT (min)
Thai	6.86	2.04	1.64	3.36	B	19.3	10.4
Thaibonnet	7.11	2.06	1.73	3.45	B	20.0	12.1
Basmati	6.85	1.77	1.53	3.88	B	16.3	9.5
Surinam	7.73	2.30	1.61	3.36	B	22.4	12.7
Ariete	6.22	2.55	1.84	2.44	A	22.2	14.3
Selenio	3.96	2.88	1.95	1.38	S	19.6	13.8
Saturno	7.04	2.09	1.69	3.37	B	22.4	12.8
Sillaro	6.84	2.17	1.76	3.16	B	23.3	12.1
Eolo	7.02	2.08	1.66	3.38	B	22.0	11.7
Aychade	7.26	2.08	1.65	3.49	B	22.4	12.3
Gacholle	6.68	2.10	1.60	3.18	B	20.0	11.1
Mistral	6.94	2.26	1.73	3.07	B	23.7	13.7
Fidji	7.13	2.09	1.66	3.41	B	22.0	12.5
Thaibonnet	7.05	2.03	1.73	3.47	B	22.3	10.6
Gladio	6.73	2.14	1.76	3.15	B	22.1	12.9
Guixel	7.42	2.04	1.64	3.64	B	22.1	12.6
Gallis	6.85	1.97	1.61	3.48	B	19.8	11.2
Soulanet	6.99	2.12	1.71	3.30	B	22.7	11.6
Adriano	7.20	2.13	1.73	3.38	B	23.5	12.5
Aurelia	7.30	2.06	1.76	3.55	B	23.4	13.1
Sambuc	7.54	2.22	1.77	3.40	B	26.5	12.1
Ruille	6.91	2.32	1.73	2.98	A	23.9	13.1
Bravo	6.23	2.73	1.82	2.28	A	26.4	14.7
Tamarin	6.72	2.42	1.86	2.78	A	26.3	15.4
Faraman	6.80	2.54	1.77	2.68	A	26.3	13.2
Selenio	4.64	2.78	1.94	1.67	S	20.8	12.1
Cigalon	5.02	2.87	1.94	1.75	S	23.0	12.0

	chemical composition (% db)					starch thermal properties		
variety	proteins	amylose	ash	β-glucans	arabinoxylans	T_0 (°C)	ΔH (J/g bs)	CX (J/g bs)
Thai	7.5	13.9	0.68	0.040	0.22	61.9	13.5	0.55
Thaibonnet	7.5	23.9	0.86	0.053	0.23	65.9	12.8	2.98
Basmati	9.6	22.8	0.65	0.065	0.22	65.5	12.7	1.24
Surinam	8.8	23.4	0.49	0.088	0.24	55.9	13.1	0.80
Ariete	7.4	18.4	0.95	0.062	0.22	59.7	13.5	1.44
Selenio	6.0	18.8	0.59	0.054	0.21	57.4	12.9	2.19
Saturno	7.5	15.0	0.35	0.070	0.21	73.8	15.5	0.34
Sillaro	7.6	26.4	0.51	0.073	0.18	70.1	12.4	0.89
Eolo	6.9	25.8	0.56	0.060	0.22	71.0	10.5	0.71
Aychade	8.5	22.8	0.60	0.140	0.22	68.3	12.7	0.74
Gacholle	7.5	15.8	0.56	0.124	0.22	63.8	13.9	1.39
Mistral	7.6	15.7	0.48	0.100	0.20	62.8	12.6	0.85
Fidji	6.4	18.0	0.37	0.098	0.21	59.5	13.4	1.50
Thaibonnet	6.0	26.4	0.35	0.067	0.24	71.3	11.4	0.71
Gladio	7.9	26.5	0.40	0.066	0.17	71.2	11.8	0.85
Guixel	10.5	25.8	0.58	0.069	0.22	70.4	11.9	0.62
Gallis	7.1	21.7	0.32	0.109	0.21	69.9	12.9	0.65
Soulanet	5.6	14.6	0.19	0.104	0.19	61.3	14.1	1.06
Adriano	7.9	25.1	0.21	0.071	0.21	71.3	10.5	0.92
Aurelia	7.6	13.6	0.34	0.072	0.24	74.0	15.1	0.32
Sambuc	7.3	14.3	0.36	0.137	0.19	63.4	15.0	0.99
Ruille	7.0	13.0	0.30	0.075	0.19	61.8	14.4	1.07
Bravo	8.1	15.9	0.38	0.094	0.17	63.6	13.0	1.25
Tamarin	7.7	16.0	0.31	0.112	0.18	63.3	14.0	0.90
Faraman	8.0	14.9	0.25	0.125	0.19	61.2	12.8	0.94
Selenio	7.0	14.7	0.22	0.079	0.23	64.1	13.5	1.14
Cigalon	8.1	15.8	0.24	0.093	0.21	64.9	12.1	1.18

[a] *L*, *W*, and *T*: length, width, and thickness of rice kernel; TKW: thousand kernel weight; CT: cooking time. T_0, ΔH: gelatinization onset and enthalpy change; CX: enthalpy of complexes between amylose and lipids.

samples with extreme amylose content and T_o values, respectively 13.6 to 25.5% (db) and 59.5 to 74.0 °C. Most samples had an amylose/lipid complex melting enthalpy around 1 J/g (db; **Figure 5d**), but two commercial samples had double this value.

Ash content was distributed from 0.19 to 0.68% (db), except for two commercial samples with 0.86 and 0.95%. The amount of arabinoxylans did not vary greatly, ranging from 0.17 to 0.24% (db). β-D-glucan content, however, exhibited a large variation, from 0.05 to 0.14% (db), with a mean value of around 0.08%.

Cooking tests were performed for each cultivar, starting with a cooking time of 8 min and then staggering every 30 s. Cooking time for attaining a swelling ratio of 2.55 was calculated from the regression model between time and swelling ratio. It ranged from 9.5 min to 15.4 min (**Table 3**).

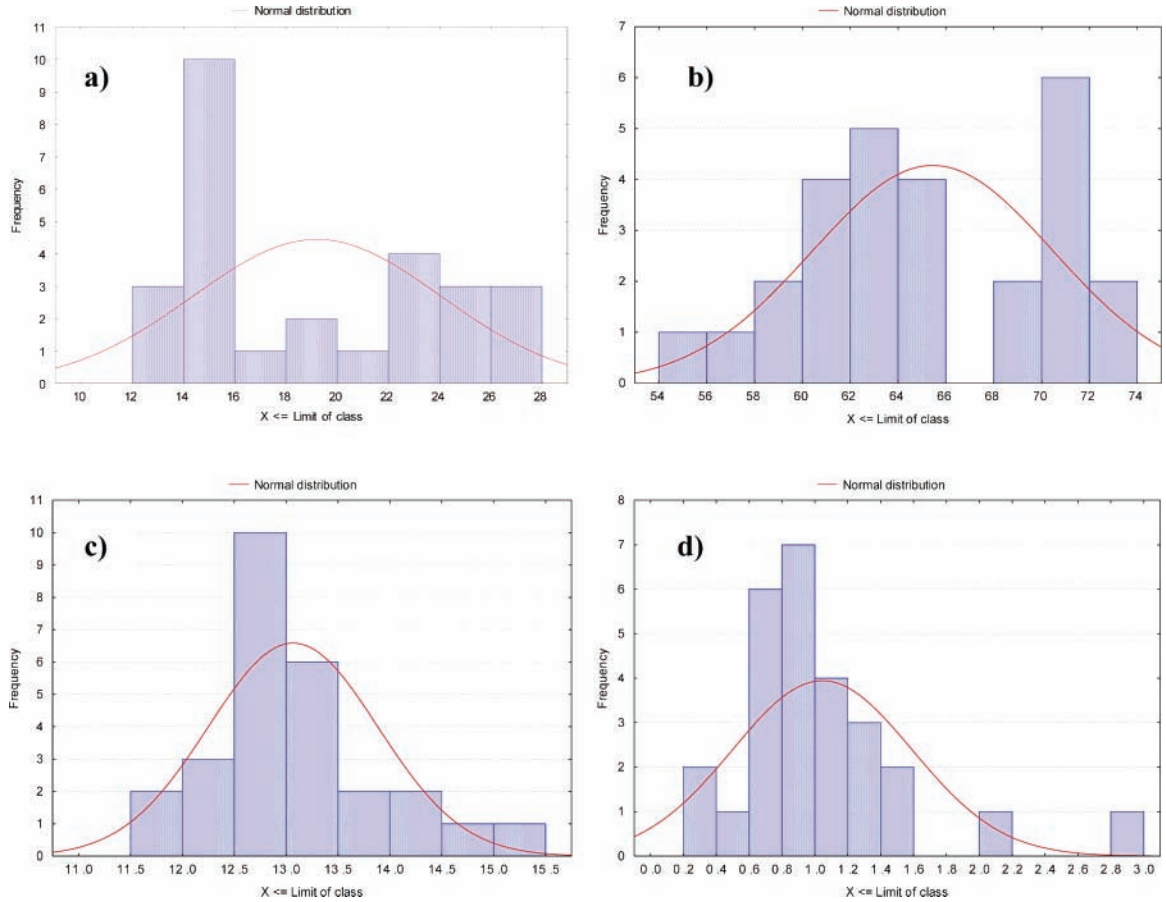

Figure 5. Histogram of the distribution of amylose content (a), gelatinization onset temperature (b), gelatinization enthalpy (c), and fusion enthalpy of amylose–lipid complex (d).

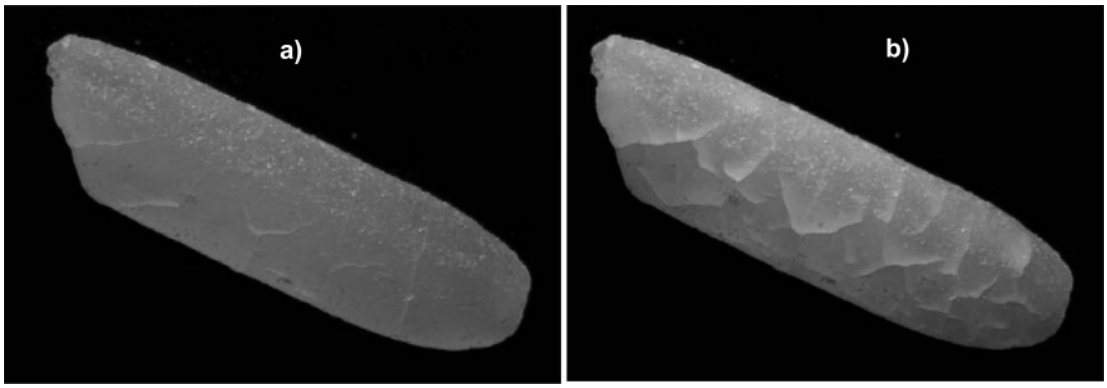

Figure 6. Raw milled rice kernel observed under stereomicroscope with magnification of 10×: (a) at the start of illumination, and (b) 5 min later.

Microscopy. Microscopic studies were performed on a limited sample, comprising long A and B and short grains.

Raw rice kernels were viewed directly under a stereomicroscope (**Figure 6**). Fractures appeared on the surface within a few minutes' exposure to light. The shape and the number of fractures seemed to vary according to the rice cultivar. We were however unable to assess this phenomenon.

Raw rice fractures obtained after bending until breaking point were observed by SEM at low magnification (**Figure 7**). The fracture partly passes between cells as revealed by a smooth polygonal surface. It could also pass through cells revealing a rough surface. The proportion of smooth to rough surface varies according to the cultivar; with one cultivar (Aurelia), most cells appeared fractured (**Figure 7c**). These observations were confirmed by duplicated fractures for each cultivar.

The axis of the grain seemed to be at the center of the grain section for long type cultivars (Gachole or Thaibonnet) but closer to the ventral part of the grain for short grain type cultivars (Selenio). The cells were elongated and polygonal, arranged radially. They appeared longer in the intermediate zone (approximately 150 μm long) than in the central zone (less than 50 μm long). They seemed longer and thinner in short grain than in long grain cultivars. Cell walls appeared very thin, revealing closely packed amyloplasts (**Figure 8**) composed of closely packed polygonal starch granules (**Figure 9**). It was not possible to evaluate cell wall thickness on SEM images due to the thinness.

These structural features were confirmed by confocal laser scanning microscope observations of cross-sections (**Figure 10**). Elongated cells in the intermediate zone were approximately 150 μm long whereas central cells were much shorter. At higher magnitude (**Figure 11**), cell walls could be viewed and their

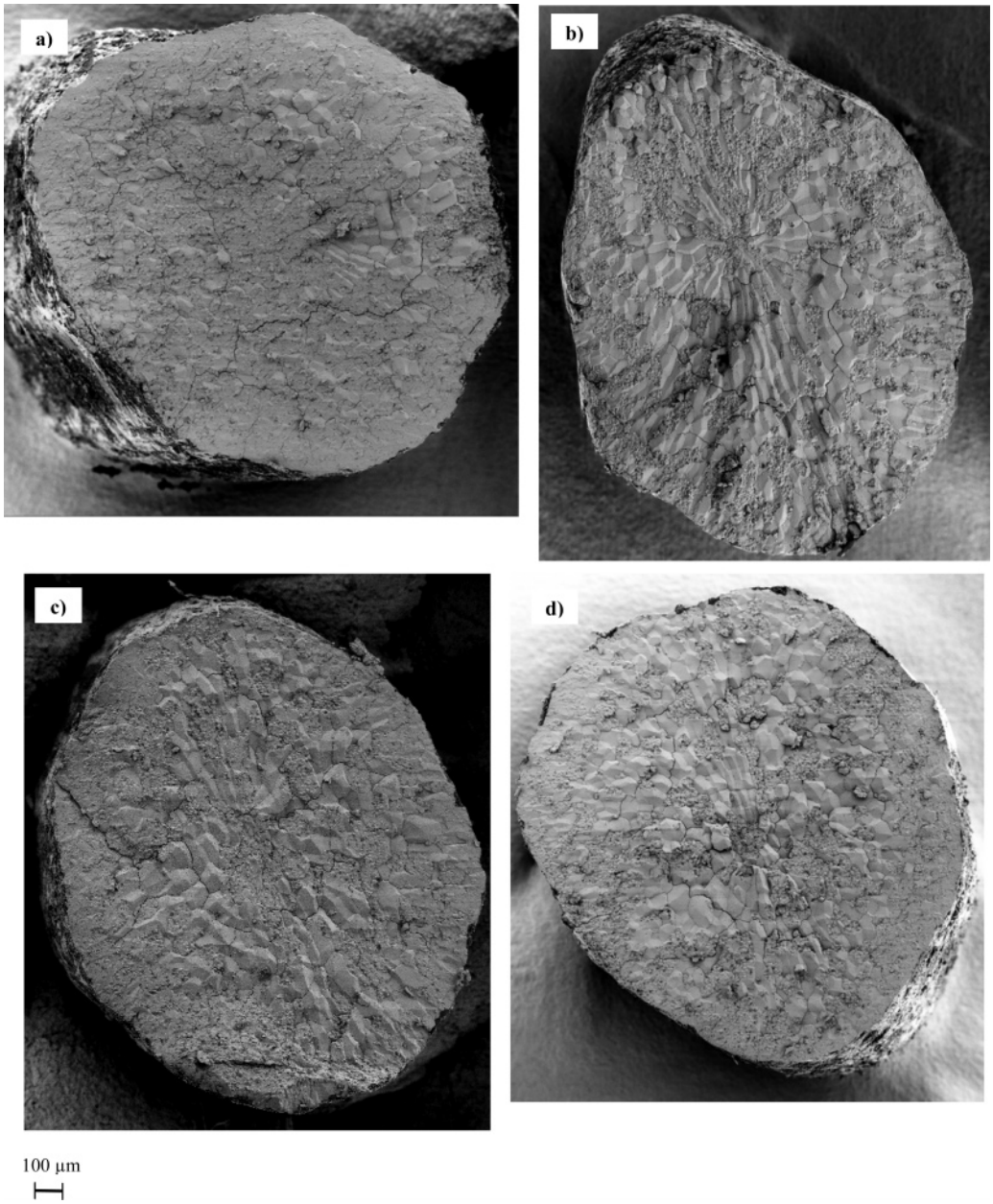

Figure 7. Raw milled rice kernel fractures observed by SEM at a magnification of 120×: Aurelia (a), Selenio (b), Gachole (c), and Thaibonnet (d).

thickness estimated at under 1 μm. Starch granules are small (around 5 μm and under) compacted in amyloplasts (18 μm wide approximately). Amyloplasts are also packed together in cells that are squeezed in the endosperm.

DISCUSSION

Cooking Time. Ranghino (*4*) first defined rice cooking time as the time necessary for 90% of the kernels to be completely translucent when cooked in distilled water at 96 °C (±1 °C) immersed in a boiling saucepan. Juliano et al. (*5*) preferred to call it minimum cooking time, adding 2 min to obtain optimum cooking time. Bhattacharya and Sowbhagya (*9*) proposed the cooking end time as when all the kernels become translucent: they then obtained a swelling ratio ranging from 3.1 to 3.5. Mohapatra and Bal (*10*) used the procedure of Juliano et al. (*5*) to determine optimum cooking time: a swelling ratio of 3−3.2 for a 12% milled rice, equivalent to the one used in this study. We also observed that 100% kernel translucence at a swelling ratio of around 3.

We chose a cooking time corresponding to an incomplete but fixed starch gelatinization level (95%) corresponding to a fixed swelling ratio of 2.55. This level of cooking is lower than the one used in an international comparative study (complete translucence and a swelling ratio ranging from 3.4 to 4.0; *5*). On the other hand, it has also been proposed to conduct intercomparison cooking tests with a constant swelling ratio of 2.6 (*6*), or with a swelling ratio adapted to grain type (from 2.0 for waxy rice to 3.0 for high-amylose rice). The latter condition reduced the textural differences between samples, and so we preferred to cook all rice cultivars to the same cooking (gelatinization) level, in order to maintain as great a textural diversity as possible. Partly undercooked rice would enable better distinction.

Physicochemical Characteristics. Amylose and protein contents were in the range encountered in short to long grain rice populations (*11*). Gelatinization onset temperature (T_0) was also in the same range as previously reported (*12*, *13*, *14*). Gelatinization enthalpy (ΔH) was however higher than in the

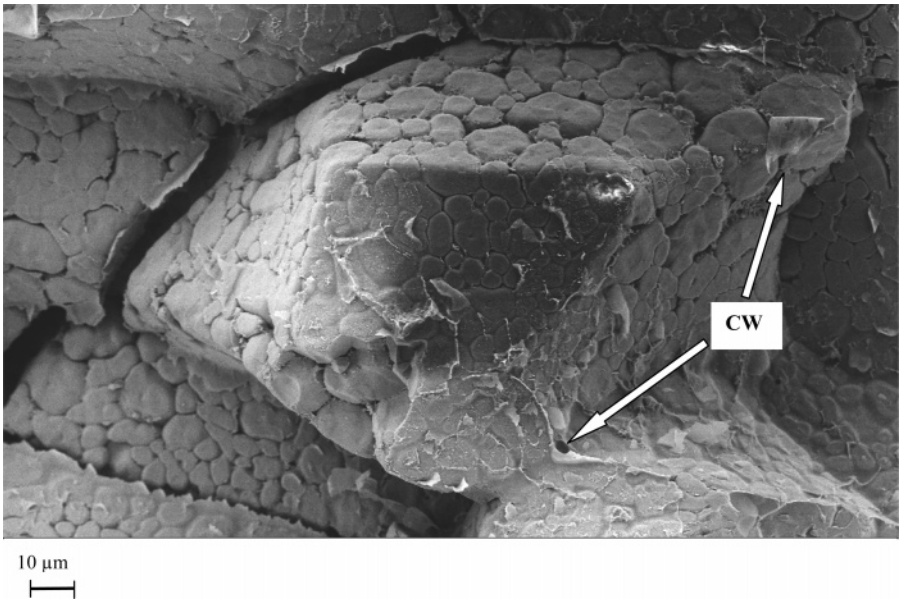

Figure 8. Raw milled rice fracture observed by SEM at a magnification of 1800 (CW, cell wall).

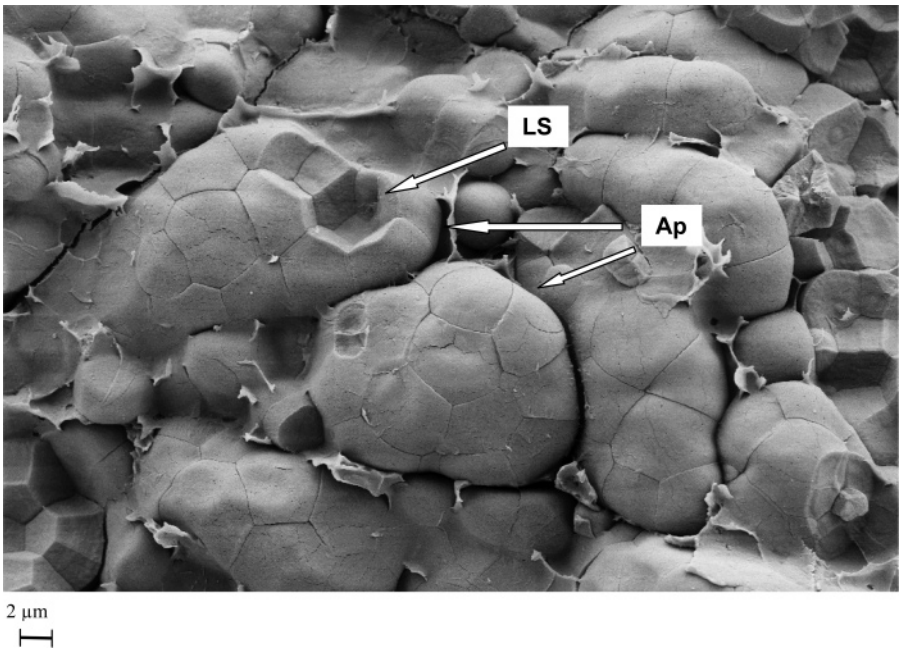

Figure 9. Raw milled rice fracture observed by SEM at a magnification of 7000 (Ap, amyloplast; LS, lacking starch granule).

literature (3.0−11.2 J/g). This difference was certainly due to the experimental measurement conditions: we used a higher water/rice ratio (5) than used by other authors (2−2.5), which maximized the gelatinization enthalpy (*15*). Amylose−lipid complex fusion is rarely documented in rice. These complexes are formed between amylose and free fatty acids or starch monoacyl lipids (*16*). They melt above 100 °C (*17*, *18*) with enthalpies (named CX) varying between 0.2 and 0.6 J/g. Most samples gave values in this range, except two commercial samples. This may have been due to longer storage time, which promotes free fatty acid release and complex ability (*19*). The age of these samples, collected from the supermarket, was actually unknown, and they were stored in laboratory 6 months longer than the other samples.

Cell wall proportion and composition in rice is still in debate. Cell walls are a very minor component of rice endosperm, with 0.3 to 0.7% of endosperm (*20*, *21*) which is much less than for other cereals such as wheat (around 3%, *22*) or maize (around 1.5%, *23*). Cellulose and hemicelluloses are the main fraction (27−50%) of cell walls, the latter being mainly composed of arabinoxylans. We found a mean arabinoxylan content of 0.20% (db) which accounts for an estimated 20 to 60% of the cell wall. This is in the range of the previous studies. β-D-glucan content varied greatly between cultivars. The range overlapped the value (0.13% db) obtained by Anderson et al. (*24*) for one cultivar. Arabinoxylan was much more abundant than β-D-glucan: the ratio of arabinoxylan to β-D-glucan ranged between 1.4 and 5.6. By comparison, Pascual and Juliano (*25*) estimated β-D-glucan content at roughly 20% of rice endosperm cell wall, not so far from the heteroxylan proportion (∼27%). However, they estimated the β-D-glucan content from the glucose abundance in the 4 M KOH soluble fractions, and this value could be overestimated due to the presence of residual starch which can contaminate cell wall preparation. The sum of arabinoxylan and β-D-glucan accounted for 0.25 to 0.35% of dry matter, which is consistent with the estimated cell wall proportion in rice (0.3

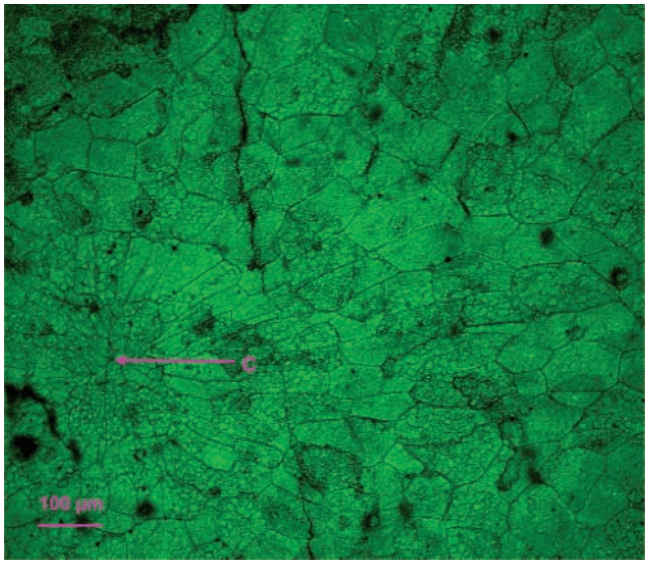

Figure 10. Raw milled rice fracture observed by CLSM (C, center of the grain).

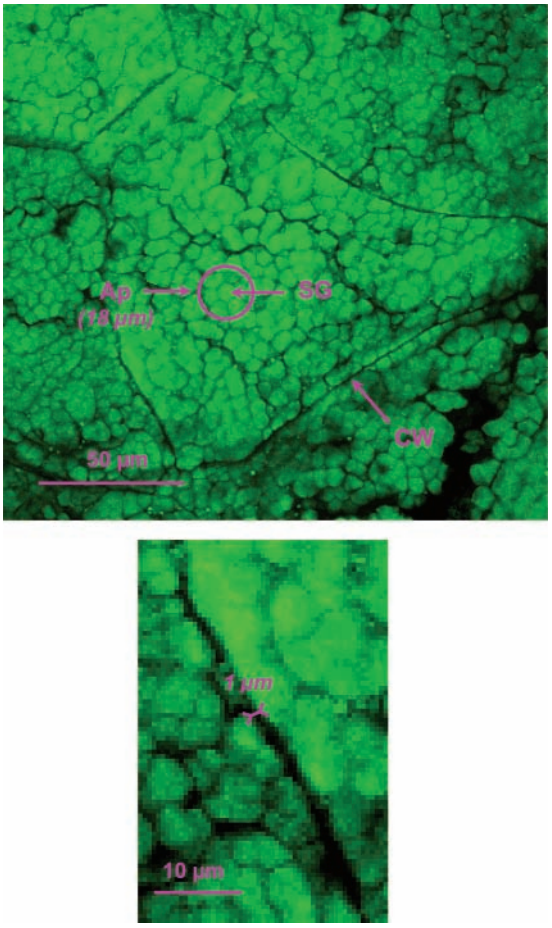

Figure 11. Raw milled rice fracture observed by CLSM (Ap, amyloplast; SG, starch granule; CW, cell wall).

to 0.7%). Ash contents were in the range generally mentioned for milled rice (0.3−0.8% db; *26*). The higher values observed for two commercial samples may be due to undermilling, as bran is much richer in ash. However, these samples were not the richest in cell wall components, and contamination during the industrial milling operation may also explain this result.

Principal Component Analysis. A principal component analysis was carried out to extract the main variables describing the rice kernel diversity and to better understand the complex relationships between the different variables. The first four factors accounted for 75% of the total variance. Factors 1 and 2 explained the largest proportion of the variance: 30.1% and 21.5% respectively. Factor 1 was mainly associated with the morphological parameters (**Figure 12**): W and T were the most closely associated parameters, with a correlation coefficient higher than 0.83 (**Table 4**). L, on the other hand, had a negative weighting on the first factor, together with amylose and Tonset variables. Morphological (TKW and L) and chemical (ash, β-glucan and CX) variables were associated with factor 2. Factor 3 explained 14% of variance and was positively influenced by ΔH. Factor 4, which explained 10% of variance, was negatively influenced by the protein content.

A clear topological separation was revealed on the first plan (**Figure** 13). B-Type cultivars were located on the left portion of the graph whereas short grains were in the bottom-right. Besides the shape variables, most B-type cultivars were located in the vicinity of Tonset and amylose variables and opposite the CX variable. B-Type cultivars were the only ones with high Tonset (over 65 °C), high amylose content (over 21% db), and

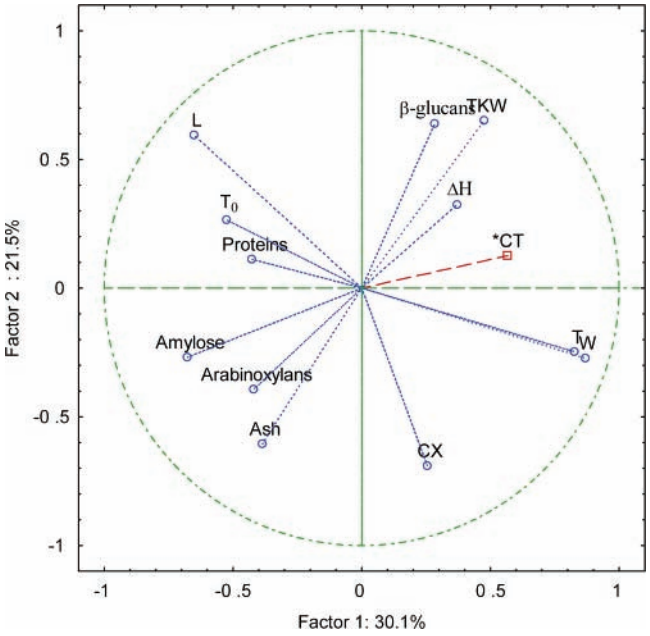

Figure 12. Principal component plot on the first two axes for the physicochemical variables; cooking time is plotted as an additional variable.

Table 4. Weightings of the Variables on the First Four Principal Components[a]

	factor 1	factor 2	factor 3	factor 4
L	–0.65	0.59	0.19	–0.20
W	0.87	–0.27	-0.24	–0.10
T	0.83	–0.25	-0.36	0.12
TKW	0.48	0.65	-0.30	–0.24
proteins	–0.43	0.11	-0.12	–0.48
amylose	–0.68	–0.27	-0.55	–0.21
ash	–0.39	–0.61	0.31	–0.38
β-glucans	0.28	0.64	0.16	–0.35
arabinoxylans	–0.42	–0.39	0.31	0.41
T_0	–0.53	0.27	-0.46	0.44
ΔH	0.37	0.32	0.73	0.18
CX	0.26	–0.69	0.17	–0.37
CT	0.57	0.13	–0.19	–0.29

[a] *L*, *W*, and *T*: length, width, and thickness of rice kernel; TKW: thousand kernel weight; T_0, ΔH: gelatinization onset and enthalpy change; CX: enthalpy of complexes between amylose and lipids; CT: cooking time.

Table 5. Correlation Coefficients between Physicochemical Characteristics and Cooking Time[a]

	L	W	T	TKW	proteins	amylose	ash	β-glucans	arabinoxylans	T_0	ΔH	CX
L	1											
W	–0.78 ***	1										
T	–0.74 ***	0.87* **	1									
TKW	0.20	0.35	0.39*	1								
proteins	0.28	–0.17	–0.33	–0.04	1							
amylose	0.25	–0.40 *	–0.32	–0.28	0.27	1						
ash	0.05	–0.19	–0.23	–0.47*	0.24	0.30	1					
β-glucans	0.20	0.07	–0.06	0.48*	0.02	–0.30	–0.3 9*	1				
arabinoxylans	0.04	–0.24	–0.26	–0.54 **	0.04	0.14	0.31 *	–0.31	1			
T_0	0.29	–0.48*	–0.20	–0.02	0.17	0.41*	–0.1 6	–0.18	0.10	1		
ΔH	0.05	0.05	0.06	0.15	–0.17	–0.76* **	–0.1 0	0.27	–0.06	–0.2 4	1	
CX	–0.39*	0.29	0.28	–0.26	–0.21	0.05	0.42 *	–0.15	0.02	–0.4 5*	–0. 06	1
CT	–0.18	0.58* *	0.57* *	0.66* **	–0.01	–0.26	–0.0 7	0.14	–0.42*	–0.2 3	0.1 9	0.0 9

[a] *Significant at 5% level. **Significant at 1% level. ***Significant at 0.1% level. *L*, *W*, and *T*: length, width, and thickness of rice kernel; TKW: thousand kernel weight; T_0, ΔH: gelatinization onset and enthalpy change; CX: enthalpy of complexes between amylose and lipids; CT: cooking time.

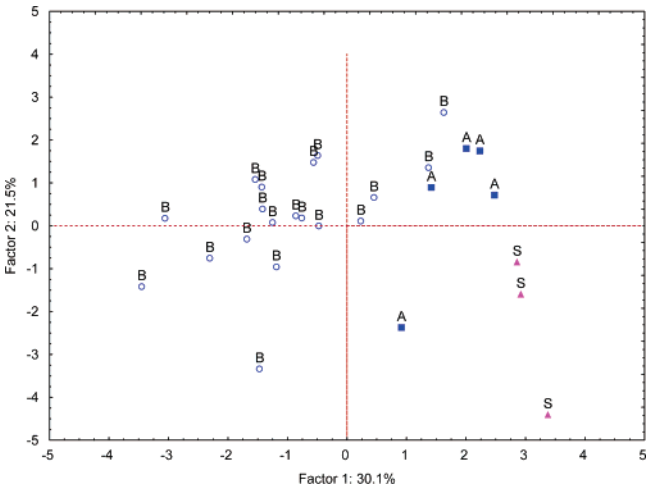

Figure 13. Scatter plot scores of rice varieties for the first two principal components.

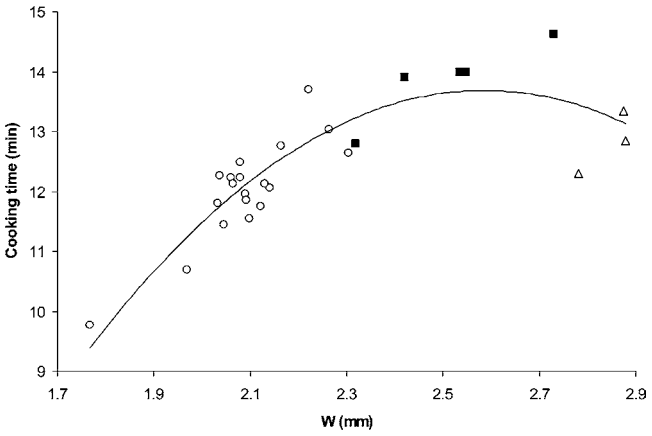

Figure 14. Regression between cooking time and rice kernel width: (○), B-type rice kernels; (■), A type rice kernels; (△), short type kernels.

low CX (less than 0.9 J/G db). Long grain cultivars are indeed generally characterized by relatively high amylose contents and intermediate to high gelatinization temperature (*27*). It should however be noted that only some (almost half) B-type cultivars exhibited these unique features, while the others were not distinct from the other rice types. Strangely, a single cultivar seldom exhibited all these features, and the correlation between amylose content and Tonset was very weak (**Table 5**). On the other hand, A-type cultivars and short grains were mainly located on the right and were characterized by high kernel weight and

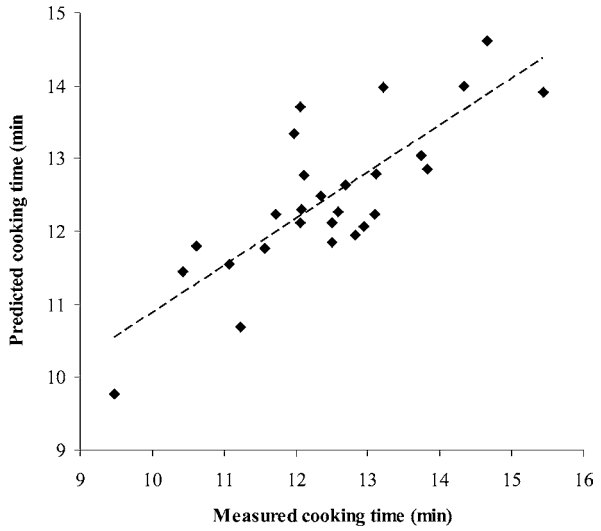

Figure 15. Regression between measured and predicted cooking time values.

gelatinization enthalpies but low amylose and ash contents. Amylose content and gelatinization enthalpy were negatively correlated (−0.76), which was consistent with the previous study of Biliaderis et al. (*28*), but did not agree with the results of Tan and Corke (*12*). It should be noted that the two separated cultivars A and B (at the bottom of the graph) were the commercial samples with high ash content and amylose complex level.

Structure. SEM and CLSM images confirmed the radial cell orientation in rice endosperm and the larger size in short grain cultivars already observed by Juliano and Bechtel (*29*). Starch granules were never observed in isolation, but in 18 μm large amyloplasts. Accordingly, Fitzgerald (*30*) observed amyloplasts of at least 16 starch granules, with their size ranging between 7 and 39 μm (*20*). Fracturing due to bending revealed a significant variety of raw rice kernel mechanical behavior. Some cultivars had a completely rough fracture whereas others exhibited a large smooth portion. The rough surface resulted from cell opening. This indicates that cell−cell adhesion was greater than the cell wall strength, resulting in cell wall rupture (*31*). So it would be interesting to assess the impact of this phenomenon and try to relate it with rice cooking behavior.

As already observed (*26*), cell walls are very thin in rice endosperm cells and are difficult to see with SEM. Cell wall thickness could only be estimated by CLSM at 1 μm, and we were not able to reveal any difference between cultivars in this

property. This very low thickness was consistent with the very low cell wall yield. There was however no direct relationship between cell wall composition and fracturing behavior: the cultivar with a completely rough surface had a high arabinoxylan content, together with another cultivar which had a smooth fracture. This mechanical difference may indeed be due to another cell wall component present in rice (*21*), pectins, which play a role in cell adhesion and the crispness of apples, for example (*32*).

Cracks rapidly appeared at the surface of rice kernel exposed to dry air. Ogawa et al. (*33*) also observed cracks by SEM on dry-fracture cross sections. This phenomenon grows during cooking, leading to vacuum formation in the kernel. This would facilitate water absorption and kernel swelling during cooking. So it should be interesting to assess crack formation capacity and try to relate it with swelling capacity and cooking time.

Predictive Equation To Determine Optimum Cooking Time. Optimum cooking time was plotted on the PCA as an additional variable (not participating in the definition of the axes). It appeared mainly, but quite poorly, correlated with the first axis (**Figure 12**, **Table 4**). It was indeed primarily correlated with the geometrical (size and shape) kernel characteristics (**Table 5**). Cooking time increased proportionally with the width until a maximum around 2.7 mm and decreased beyond (**Figure 14**). Long B-type grains were located in the linear part of the curve, whereas long A-type grains were on the plateau and short rice on the descent of the curve. So short grains had a shorter cooking time than expected from their geometrical characteristics. Kernel defects (such as cracks, chalky cores), structural features (such as size and shape of endosperm cells), or chemical composition should play a part in explaining cooking time.

In this way a multiple regression model was developed. The best model could predict 64% of cooking time variability (**Figure 15**):

$$\text{CT (min)} = -0.81 + 1.79 \times W + 0.37 \times \text{TKW} + 2.16 \times \text{ash}$$

where CT is cooking time, W the width (mm), TKW the thousand kernel weight (g db), and ash the ash content (% db).

The regression factor was positive for ash content. This could be linked to the degree of milling. In a recent report, Mohapatra and Bal (*10*) in fact revealed that the degree of milling (and conversely the ash content) was negatively correlated with cooking time. No other physicochemical property fitted in the model. This implied that optimum cooking time was mainly linked to grain morphology and to degree of milling but not to starch properties such as amylose content or gelatinization temperature. Previous studies reported that the optimum cooking time determined for a swelling ratio of 2.5 was primarily related to the grain surface area per unit weight (*9*, *34*).

As per Bhattacharya and Sowbhagya (*9*), we did not find any correlation between amylose content and cooking time. However, contradictory results have been obtained concerning the relationship between starch properties and rice cooking behavior. Singh et al. (*35*) found a negative correlation between cooking time and amylose content, whereas Sowbhagya et al. (*34*) found a negative correlation of amylose content with rice kernel swelling capacity at 70 °C but a positive correlation for the swelling capacity at 96 °C. Starch gelatinization temperature was also found to be highly correlated with cooking time (*36*), determined by the adapted Ranghino method, in particular for rice kernels of similar morphology (*37*).

The model could only explain 64% of cooking time variability. Other parameters, not measured in this study, must contribute to rice kernel swelling and cooking capacity. This could be the toughness of the cell wall; a large variability was indeed revealed under the microscope. So it could be interesting to quantify the proportion of opened cells after standardized rupturing, to evaluate cell wall toughness. Another approach should be to assess the pectin content, as these components are quantitatively quite high in rice (*38*) and are generally thought to be involved in the cell adhesion phenomenon (*32*). The positive relationship between cooking time and ash content also tends to point to the possible role of pectins, since these components are very rich in minerals.

ABBREVIATIONS USED

L, W, and T, length, width, and thickness of rice kernel; TKW, thousand kernel weight; DSC, differential scanning calorimetry; T_o, ΔH, gelatinization onset and enthalpy change; CX, enthalpy of complexes between amylose and lipids; SEM, scanning electron microscopy; CLSM, confocal laser scanning microscopy; CT, cooking time; SR, swelling ratio.

ACKNOWLEDGMENT

We are grateful to Didier Louvel (CFR) for supplying rice samples. The help of Anne Surget (INRA) in cell wall component analyses is fully acknowledged. The support by Béatrice Condé-Petit and Felix Escher, ETH Zürich, is also acknowledged.

LITERATURE CITED

(1) Lyon, B. G.; Champagne, E. T.; Vinyard, B. T.; Windham, W. R. Sensory and instrumental relationships of texture of cooked rice from selected cultivars and postharvest handling practices. *Cereal Chem.* **2000**, *77*, 64−69.

(2) Okabe, M. Texture measurement of cooked rice and its relationship to the eating quality. *J. Texture Stud.* **1979**, *10*, 131−152.

(3) Rousset, S.; Pons, B.; Martin, J.-M. Identifying objective characteristics that predict clusters produced by sensory attributes in cooked rice. *J. Texture Stud.* **1999**, *30*, 50−532.

(4) Ranghino, F. Valutazione delle resistenza del riso alla cottura, in base al tempo di gelatinizzazione dei granelli. *Il Riso* **1966**, *15*, 117−127.

(5) Juliano, B. O.; Perez, C. M.; Barber, S.; Blakeney, A. B.; Iwasaki, T.; Shibuya, N.; Keneaster, K.; Chung, S. O.; Laignelet, B.; Launay, B.; Del, Mundo, A.; Suzuki, H.; Shiki, J.; Tsuji, S.; Tokoyama, J.; Tatsumi, K.; Webb, B. D. International cooperative comparison of instrument methods for cooked rice texture. *J. Texture Stud.* **1981**, *12*, 17−38.

(6) Bergman, C. J.; Bhattacharya, K. R.; Ohtsubo, K. Rice end-use quality analysis. In *Rice Chemistry and Technolgy*; Champagne, E. T., Ed.; American Association of Cereal Chemists: St. Paul, MN, 2004; pp 415−472.

(7) Rouau, X.; Surget, A. A rapid semi-automated method for the determination of total and water-extractable pentosans in wheat flours. *Carbohydr. Polym.* **1994**, *24*, 123−132.

(8) Mestres, C.; Matencio, F.; Pons, B.; Yajid, M.; Fliedel, G. A rapid method for the determination of amylose content by using Differential Scanning Calorimetry. *Starch* **1996**, *48*, 2−6.

(9) Bhattacharya, K. R.; Sowbhagya, C. M. Water uptake by rice during cooking. *Cereal Sci. Today* **1971**, *16*, 420−424.

(10) Mohapatra, D.; Bal, S. Cooking quality and instrumental textural attributes of cooked rice for different milling conditions. *J. Food Eng.* **2005**, *73*, 253−259.

(11) Bett-Garber, K. L.; Champagne, E. T.; McClung, A. M.; Moldenhauer, K. A.; Linscombe, S. D.; McKenzie, K. S. Categorizing rice cultivars based on clustur analysis of amylose content, protein content and sensory attributes. *Cereal Chem.* **2001**, *78*, 551−558.

(12) Tan, Y.; Corke, H. Factor analysis of physicochemical properties of 63 rice varieties. *J. Sci. Food Agric.* **2002**, *82*, 745−752.
(13) Sodhi, N. S.; Singh, N. Morphological, thermal and rheological properties of starches separated from rice cultivars grown in India. *Food Chem.* **2003**, *80*, 99−108.
(14) Cameron, D. K.; Wang, Y.-J. A better understanding of factors that affect the hardness and stickiness of long-grain rice. *Cereal Chem.* **2005**, *82*, 113−119.
(15) Eliasson, A. C. Effect of water content on the gelatinization of wheat starch. *Starch* **1980**, *32*, 270−272.
(16) Osman, E. M.; Leith, S. J.; Fles, M. Complexes of amylose with surfactants. **1961**, 449−463.
(17) Biliaderis, C. G.; Tonogai, J. R.; Perez, C. M.; Juliano, B. O. Thermophysical properties of milled rice starch as influenced by variety and parboiling method. *Cereal Chem.* **1993**, *70*, 512−516.
(18) Ong, M. H.; Blanshard, J. M. V. The significance of starch polymorphism in comercially produced parboiled rice. *Starch* **1995**, *47*, 7−13.
(19) Mestres, C.; Nago, M.; Akissoë, N.; Matencio, F. End use quality of some African corn kernels. 2. Cooking behavior of whole dry-milled maize flours; incidence of storage. *J. Agric. Food Chem.* **1997**, *45*, 565−571.
(20) Juliano, B. O. Polysaccharides, proteins and lipids of rice. In *Rice: Chemistry and technology*; Juliano, B. O., Ed.; American Association of Cereal Chemists: St. Paul, MN, 1985; pp 59−174.
(21) Shibuya, N.; Nakane, R.; Yasui, A.; Tanaka, K.; Iwasaki, T. Comparative studies on cell wall preparations from rice bran, germ and endosperm. *Cereal Chem.* **1985**, *62*, 252−258.
(22) D'Appolonia, B. L.; Gilles, K. A.; Osman, E. M.; Pomeranz, Y. Carbohydrates. In *Wheat, chemistry and technology*; Pomeranz, Y., Ed.; American Association of Cereal Chemists: St. Paul, MN, 1964; pp 301−392.
(23) Watson, S. A. Structure and composition. In *Corn: chemistry and technology*; Watson, S. A., Ramstad, P. E., Eds.; American Association of Cereal Chemists: St. Paul, MN, 1987; pp 53−82.
(24) Anderson, M. A.; Cook, J. A.; Stone, B. A. Enzymatic determination of 1,3:1,4-β-glucans in barley grain and other cereals. *J. Inst. Brew.* **1978**, *84*, 233−239.
(25) Pascual, C. G.; Juliano, B. O. Properties of cell wall preparations of milled rice. *Phytochemistry* **1983**, *22*, 151−159.
(26) Champagne, E. T.; Wood, D. F.; Juliano, B. O.; Bechtel, D. B. The rice grain and its gross composition. In *Rice Chemistry and Technolgy*; Champagne, E. T., Ed.; American Association of Cereal Chemists: St. Paul, MN, 2004; pp 77−107.
(27) Webb, B. D. Criteria of rice quality in the United States. In *Rice : chemistry and technology AACC Monograph Series (USA*); Juliano, B. O., Ed.; American Association of Cereal Chemists: St. Paul, MN, 1985; pp 402−442.
(28) Biliaderis, C. G.; Page, C. M.; Maurice, T. J.; Juliano, B. O. Thermal characterization of rices starches: a polymeric approach to phase transitions of granular starch. *J. Agric. Food Chem.* **1986**, *34*, 6−14.
(29) Juliano, B. O.; Bechtel, D. B. The rice grain and its gross composition. In *Rice: Chemistry and technology*; Juliano, B. O., Ed.; American Association of Cereal Chemists: St. Paul, MN, 1985; pp 17−57.
(30) Fitzgerald, M. Starch. In *Rice: Chemistry and Technolgy*; E. T. Champagne, Ed.; American Association of Cereal Chemists: St. Paul, MN, 2004; pp 109−141.
(31) Brunnschweiler, J. *Structure and texture of yam (Dioscorea spp.) and processed yam products*; Swiss Federal Institute of Food Technology: Zürich, 2004.
(32) Parker, C. C.; Parker, M. L.; Smith, A. C.; Waldron, K. W. Pectin Distribution at the Surface of Potato Parenchyma Cells in Relation to Cell-Cell Adhesion. *J. Agric. Food Chem.* **2001**, *49*, 4364−4371.
(33) Ogawa, Y.; Glenn, G. M.; Orts, W. J.; Wood, F. W. Histological structures of cooked rice grain. *J. Agric. Food Chem.* **2003**, *51*, 7019−7023.
(34) Sowbhagya, C. M.; Ramesh, B. S.; Ali, S. Z. Hydratation, swelling and solubility behavior of rice in relation to other physicochemical properties. *J. Sci. Food Agric.* **1994**, *64*, 1−7.
(35) Singh, N.; Kaur, L.; Sodhi, N. S.; Sekhon, K. S. Physicochemical, cooking and textural properties of milled rice from different Indian rice cultivars. *Food Chem.* **2005**, *89*, 253−259.
(36) Juliano, B. O. An international survey of methods used for evaluation on the cooking and eating qualities of milled rice. *Intl. Rice Res. Newsl.* **1982**, 1−28.
(37) Juliano, B. O.; Perez, C. M. Major factors affecting cooked milled rice hardness and cooking time. *J. Texture Stud.* **1983**, *14*, 235−243.
(38) Shibuya, N. *Plant cell wall polymers: biogenesis and biodegradation*; American Chemical Society: Washington DC, 1989; pp 333−344.

Received for review July 12, 2006. Revised manuscript received November 3, 2006. Accepted November 14, 2006. This work was supported by ONIC (France).

JF061945O